Title	Calculation of Nuclear Form Factors Using Method of Moment
All Authors	Cho Cho Win
Publication Type	Local publication
Publisher (Journal name, issue no., page no etc.)	Pathein University Symposium, Vol. 1, No. 5
Abstract	The nuclear form factor is the Fourier transform of the spatial charge distribution, □ (*r*) . This provides a powerful tool for determining the spatial charge extent and shape of the nuclei. The nuclear form factors for various charge distributions are analytically derived in this work. The form factors are also calculated by using the method of moment for different forms of nuclear charge distributions and compared with the other results.
Keywords	form factor, charge distribution, Method of Moment
Citation	
Issue Date	2016

Calculation of Nuclear Form Factors Using Method of Moment

Dr Cho Cho Win*

Abstract

The nuclear form factor is the Fourier transform of the spatial charge distribution, $\rho(r)$. This provides a powerful tool for determining the spatial charge extent and shape of the nuclei. The nuclear form factors for various charge distributions are analytically derived in this work. The form factors are also calculated by using the method of moment for different forms of nuclear charge distributions and compared with the other results.

Key words: form factor, charge distribution, Method of Moment

Introduction

The analysis of electron scattering data provides most valuable information about the charge distribution in atomic nuclei. Elastic electron scattering for probing nuclear structure was pioneered in 1953 at the Stanford Linear Accelerator by Hofstadter and collaborators. Elastic electron-nucleus scattering has been for many years a very useful tool to investigate the size and shape of stable nuclei. Concerning the charge distributions of nuclei, it is known that their most accurate determination can be obtained from electron-nucleus scattering. Since the nucleus is not a point particle, any mathematical treatment of scattering needs to take into account the spatial distribution of charge and mass within the nucleus. The spatial extension of a nucleus is described by the nuclear form factor. The form factor is the Fourier transformation of the nuclear density and describes the extension of the nucleus. There are several ansatz for determining the form factor by assuming typical $\rho(r)$ functions. This paper reviews briefly the basic formulas used to calculate the form factors for some typical nuclear density distributions. This paper also presents and compares the results of analytical and numerical calculations of nuclear form factors, based on tables of electron charge distributions.

* PhD, Lecturer, Department of Physics, Mandalay University

Nuclear Charge Densities and Corresponding Form Factors

The spatial extension of a nucleus is described by the nuclear form factor. The role of the nuclear form factor is easily understood by looking at the elastic scattering of electrons off nuclei (B. Povh et al., 2008). The nuclear form factor is the Fourier transform of the spatial charge distribution, $\rho(r)$ of a nucleus as

$$F(q) = \int e^{i\vec{q}\cdot\vec{r}'} \rho(\vec{r}')d^3\vec{r}' \tag{1}$$

This provides a powerful tool for determining the spatial charge distributions of the nuclei responsible for the scattering. The special case of a spherically symmetric charge distribution can be easily analyzed as

$$F(q) = 4\pi \int_0^\infty \frac{\sin(qr')}{qr'} r'^2 \rho(r')\, dr' \tag{2}$$

This expression is a useful form of the form factor. This means that for a complete knowledge of $\rho(r')$ the form factor F(q) is known for all values of the momentum transfer.

The Method of Moment for Form Factors

The sine function in equation (2) is expanded in the Taylor series,

$$\sin(qr) = qr - \frac{(qr)^3}{3!} + \frac{(qr)^5}{5!} - \frac{(qr)^7}{7!} + \ldots \tag{3}$$

and the form factor becomes

$$F(q^2) = 4\pi \int_0^\infty r^2 dr\ f(r)\left[1 - \frac{1}{3!}(qr)^2 + \frac{1}{5!}(qr)^4 - \frac{1}{7!}(qr)^6 + \ldots\right] \tag{4}$$

$$= 1 - \frac{1}{6}q^2\left\langle r^2\right\rangle + \frac{1}{120}q^4\left\langle r^4\right\rangle - \frac{1}{120}q^6\left\langle r^6\right\rangle + \ldots \tag{5}$$

$$F(q^2) = 1 + \sum_{k=1}^{\infty}(-1)^k \frac{q^{2k}}{(2k+1)!}\left\langle \boldsymbol{r}^{2k}\right\rangle \tag{6}$$

The effect of nuclear distribution on nuclear form factors then becomes proportional to the moments $\left\langle r^{2k}\right\rangle$ of the distribution. The nuclear form factors can be adequately described by the moments $\left\langle r^{2k}\right\rangle$ of the

distribution. Varying the parameter in the Fermi distribution makes it possible to study the influence of the higher nuclear moments, $\left\langle r^{2k} \right\rangle$, given to a good approximation (M. G. H. Gustavsson and A.-M. Martensson-Pendrill, 1998) by the relations

$$\left\langle r^2 \right\rangle \approx \frac{3}{5}c^2 + \frac{7}{5}\pi^2 a^2, \tag{7}$$

$$\left\langle r^4 \right\rangle \approx \frac{3}{7}c^4 + \frac{18}{7}\pi^2 a^2 c^2 + \frac{31}{7}\pi^4 a^4, \tag{8}$$

$$\left\langle r^6 \right\rangle \approx \frac{3}{9}c^6 + \frac{11}{3}\pi^2 a^2 c^4 + \frac{239}{15}\pi^4 a^4 c^2 + \frac{127}{5}\pi^6 a^6. \tag{9}$$

Model-dependent Form Factors

There are several approaches for determining the nuclear form factor by assuming nuclear density functions $\rho(r)$ of the types: e.g. homogeneously charged sphere, exponential, Yukawa, or Woods-Saxon behavior. They can be grouped into the model-dependent approaches. Another one is the model-independent approaches such as the method of moment, the Fourier-Bessel expansion, and the Sum of Gaussian expansion.

Form factor for rectangular type distribution

A simple example of a charge density for a nucleus is a uniform distribution up to a cutoff radius, R,

$$\rho(r) = \begin{cases} \dfrac{3Ze}{4\pi R^3}, & r < R \\ 0, & r > R \end{cases} \tag{10}$$

The corresponding form factor is fairly simple to calculate and is given by

$$F(q) = \frac{3}{qR} j_1(qR) \tag{11}$$

where $j_1(qR)$ is again a spherical Bessel function of the first kind.

Two-parameter Fermi (2pF) or Woods-Saxon form factor

The form of the two parameter Fermi (2pF) distribution is

$$\rho(r) = \frac{\rho_0}{e^{(r-c)/a}+1}, \tag{12}$$

where c is the half-density radius, ρ_0 is the density at r = c, and a is related to the surface thickness *t* by *t* = (4 ln3) a. The parameters c and a for different nuclei have been determined by fitting the elastic electron scattering experiments and muonic atom spectroscopy.

Proceeding now to the derivation of F(q) (L. C. Maximon and R. A. Schrack, 1966), it is obtained

$$F(q) = \frac{4\pi\rho_0}{q}\int_0^\infty \frac{r\sin qr dr}{1+e^{(r-c)/a}} = -\frac{4\pi\rho_0}{q}\cdot \mathrm{Re}\frac{\partial}{\partial q}\int_0^\infty \frac{e^{iqr}\,dr}{1+e^{(r-c)/a}} \tag{13}$$

Marking the change of variables

$$x = e^{-r/a}, b = e^{-c/a}, \beta = qa \tag{14}$$

it follows

$$F(q) = -\frac{4\pi\rho_0 a^3}{b\beta}\,\mathrm{Re}\frac{\partial}{\partial\beta}\int_0^1 x^{-i\beta}\left(1+b^{-1}x\right)^{-1}dx\cdot \tag{15}$$

The integral appearing here is one form of the hypergeometric function

$${}_2F_1(a,b;c;z) = \frac{\gamma(c)}{\gamma(b)\gamma(c-b)}\int_0^1 t^{b-1}(1-t)^{c-b-1}(1-zt)^{-a}\,dt\cdot \tag{16}$$

Thus

$$\int_0^1 x^{-i\beta}\left(1+b^{-1}x\right)^{-1}dx = (1-i\beta)^{-1}\,{}_2F_1\left(1,1-i\beta;2-i\beta;-b^{-1}\right)\cdot \tag{17}$$

Transforming the hypergeometric function in (17)

$$
\begin{aligned}
{}_2F_1(a,b;c;z) = {} & \frac{\gamma(c)\gamma(b-a)}{\gamma(b)\gamma(c-a)}(-z)^{-a}\,{}_2F_1\left(a,1-c+a;1-b+a;z^{-1}\right) \\
& + \frac{\gamma(c)\gamma(a-b)}{\gamma(a)\gamma(c-b)}(-z)^{-b}\,{}_2F_1\left(b,1-c+b;1-a+b;z^{-1}\right)
\end{aligned} \tag{18}
$$

then it becomes

$$
F(q) = -\frac{4\pi\rho_0 a^3}{\beta}\,\mathrm{Re}\frac{\partial}{\partial\beta}\left\{-\frac{1}{i\beta}\,{}_2F_1(1,i\beta;1+i\beta;-b) + \frac{\pi b^{-i\beta}}{i\sinh\pi\beta}\right\} \tag{19}
$$

where it is used of the fact that if either of its first two parameters is zero, the hypergeometric function is unity, and also that

$$
\gamma(1-i\beta)\,\gamma(i\beta) = \frac{\pi}{i\sinh\pi\beta}\cdot \tag{20}
$$

Using the power series expansion for the hypergeometric function

$$
{}_2F_1(a,b;c;z) = 1 + \frac{ab}{c}\frac{z}{1!} + \frac{a(a+1)b(b+1)}{c(c+1)}\frac{z^2}{2!} + \ldots \tag{21}
$$

it follows, for the first term in (19),

$$
-\frac{1}{i\beta}\,{}_2F_1(1,i\beta;1+i\beta;-b) = -\frac{1}{i\beta} + \frac{b}{1+i\beta} - \frac{b^2}{2+i\beta} + \ldots \tag{22}
$$

from which

$$
\mathrm{Re}\frac{\partial}{\partial\beta}\left\{-\frac{1}{i\beta}\,{}_2F_1(1,i\beta;1+i\beta;-b)\right\} = -2\beta\left[\begin{array}{l}\dfrac{b}{(1+\beta^2)^2} - \dfrac{2b^2}{(2^2+\beta^2)^2} \\ \quad + \dfrac{3b^3}{(3^2+\beta^2)^2} - \ldots\end{array}\right]\cdot \tag{23}
$$

The evaluation of the second term in (19) is straightforward

$$
\mathrm{Re}\frac{\partial}{\partial\beta}\left\{\frac{\pi b^{-i\beta}}{i\sinh\pi\beta}\right\} = \frac{-\pi}{\beta\sinh^2\pi\beta}\left[\begin{array}{l}\pi\beta\cosh(\pi\beta)\sin qc \\ -qc\sinh(\pi\beta)\cos qc\end{array}\right]\cdot \tag{24}
$$

Thus finally, substituting (23) and (24) in (19) we have, in terms of the original parameters,

$$F(q) = -\frac{4\pi\rho_0 a^3}{(qa)^2 \sinh^2(\pi qa)}\left[\pi qa \cosh(\pi qa)\sin qc - qc\cos qc \sinh(\pi qa)\right] + 8\pi\rho_0 a^3 \sum_{n=1}^{\infty}(-1)^{n-1}\frac{n e^{-\frac{nc}{a}}}{\left[n^2 + (qa)^2\right]^2}. \quad (25)$$

This expression, without the infinite series, has been given previously by Blankenbecler (R. Blankenbecler, 1957). To determine ρ_0, the limit of (25) is taken as $q \to 0$. From F(0) = 1, the left-hand side of (25) is unity, so that

$$\rho_0 = \left\{\frac{4\pi c}{3}[(\pi a)^2 + c^2] + 8\pi a^3 \sum_{n=1}^{\infty}(-1)^{n-1}\frac{n e^{-\frac{nc}{a}}}{n^3}\right\}^{-1}. \quad (26)$$

For $\langle r^2 \rangle$, substituting (25) in

$$\langle r^2 \rangle = -6\left.\frac{\partial F}{\partial (q^2)}\right|_{q=0}, \quad (27)$$

and carrying out the differentiation, it follows

$$\langle r^2 \rangle = \rho_0\left\{\frac{4\pi c}{3}[(\pi a)^2 + c^2]\left[\frac{7}{5}(\pi a)^2 + \frac{3}{5}c^2\right] + 96\pi a^5 \sum_{n=1}^{\infty}(-1)^{n-1}\frac{n e^{-\frac{nc}{a}}}{n^5}\right\}. \quad (28)$$

It is interesting to see under what conditions the summation terms appearing in these expressions can be dropped without serious effect on the accuracy of the calculation.

Helm form factor

The Helm form factor was proposed in 1956 as a simpler alternative to the Woods-Saxon form factor (R. Helm, 1956). It is derived by combining the density of a uniform sphere with a Gaussian to allow for “softer” edges to the distribution. This gives a form factor as follows

$$F(q) = \frac{3 j_1(qR)}{qR} e^{-(qs)^2/2} \tag{29}$$

$$= 3 \frac{\sin(qR) - qR\cos(qR)}{(qR)^3} e^{-(qs)^2/2}, \tag{30}$$

with j_1 being the first-order spherical Bessel function. Lewin et al.(J. D .Lewin and P. F. Smith, 1996) proposed a set of parameters which are fixed by fitting the muonic atom spectroscopy (G. Fricke, et al., 1995) as:

$$R^2 = c^2 + \frac{7}{3}\pi^2 a^2 - 5s^2 \tag{31}$$

$$c \cong 1.23A^{1/3} - 0.6 \quad fm \tag{32}$$

$$s \cong 0.9 \quad fm, \qquad a \cong 0.52 \quad fm \tag{33}$$

Model-independent Form Factors

Elastic electron scattering data allow for very precise determinations of nuclear charge densities. The model independent methods for analyzing electron scattering data and extracting nuclear charge densities were developed by several groups. Two primary methods have emerged for extracting nuclear charge density parameters in a model independent fashion: an approach in which the charge density is written as a sum of Gaussians and an alternate approach in which the charge density is written as a Fourier superposition of Bessel functions. (G. Duda, 2007)

Sum of Gaussians (SOG) expansion

In the Sum of Gaussian expansion (SOG), first introduced by Sick (I. Sick, 1974), the charge density is given as

$$\rho(r) = \sum_{i=1}^{N} A_i \left\{ e^{-[(r-R_i)/\gamma]^2} + e^{-[(r+R_i)/\gamma]^2} \right\} \tag{34}$$

where γ and R_i are parameters representing the width of the Gaussian and the nuclear radius respectively, and A_i are coefficients defined by

$$A_i = \frac{Ze\,Q_i}{2\pi^{3/2}\gamma^3(1 + 2R_i^2/\gamma^2)} \tag{35}$$

where Qi represents the fractional charge carried by the *i*th Gaussian and leads to the definition of renormalizing the charge density as

$$\sum_{i=1}^{N} Q_i = 1. \tag{36}$$

An analytical form factor can be determined for this density parameterization, which eliminates the necessity of performing numerical integration to find the form factor as in the Woods-Saxon density parameterization. Assuming spherical symmetry, the SOG form factor is

$$F(q) = e^{-q^2\gamma^2/4} \sum_{i=1}^{N} \frac{Q_i}{1 + 2R_i^2/\gamma^2} \left[\cos(qR_i) + \frac{2R_i^2}{\gamma^2} \frac{\sin(qR_i)}{qR_i} \right]. \tag{37}$$

The other model independent parameterization of nuclear charge densities that was developed is a Fourier-Bessel expansion.

Fourier-Bessel (FB) expansion

In the Fourier-Bessel expansion (FB), first introduced by Dreher et al. (Dreher, et al., 1974), the charge density is modeled as a sum of Bessel functions up to some cut-off radius R, and is assumed to be zero thereafter.

The charge density is given as

$$\begin{aligned} \rho(r) &= \sum_{\nu} a_\nu j_0(\nu\pi r/R) \quad for \quad r \le R, \\ \rho(r) &= 0 \qquad for \quad r > R \cdot \end{aligned} \tag{38}$$

where a_ν is the parameter and $j_0(x) = \frac{\sin x}{x}$ is the zeroth order Bessel function. The charge is normalized by requiring

$$4\pi \int \rho(r) r^2 dr = Ze \cdot \tag{39}$$

This expansion also has an analytical form factor and, assuming spherical symmetry, is given as

$$F(q) = \frac{\sin(qR)}{qR} \frac{\sum_{\nu=1}^{N} (-1)^\nu a_\nu / (\nu^2\pi^2 - q^2R^2)}{\sum_{\nu=1}^{N} (-1)^\nu a_\nu / \nu^2\pi^2} \tag{40}$$

which is normalized to F (0) = 1.

Results and Discussions

The form factor calculations for ^{40}Ca and ^{208}Pb of this work are based on the method of moment (MoM), the model dependent and the model independent approaches. The model dependent approach consists of nuclear densities of rectangular type distribution, two-parameter Fermi (2pF) or Woods-Saxon distribution and Helm distribution. The model independent approaches are Fourier-Bessel (FB) method and the Sum of Gaussian (SOG) method. The quantitative comparisons of the form factors squared factors for ^{40}Ca and ^{208}Pb are listed in Tables (3.1) to (3.12). The calculated results of the form factors squared for ^{40}Ca and ^{208}Pb, obtained by using these methods are shown in the Figures (3.1) to (3.12).

The form factors for ^{40}Ca and ^{208}Pb are computed at the appropriate momentum transfers from 0 to 3 fm^{-1} with two-parameter Fermi (2pF) or Woods-Saxon distribution and from 0 to 30fm^{-1} with rectangular type distribution. All figures show that there are oscillations in the form factor curves. They have dips but no zeros and are much more similar in shape.

Table (3.1) The Rectangular(MoM) and SOG form factors for ^{208}Pb

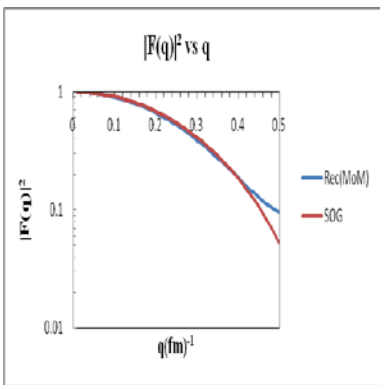

q	$\|F(q)\|^2$		
(fm^{-1})	Rectangular(MoM)	SOG	Percentage
0.1	0.9055	0.9121	0.72
0.2	0.6670	0.6860	2.77
0.3	0.3927	0.4128	7.87
0.4	0.1879	0.1856	1.22
0.5	0.0961	0.0528	45.06

Fig.(3.1)Rectangular(MoM) and SOG form factors for ^{208}P

Fig. (3.1) shows the MoM form factor with rectangular shape density distribution and SOG form factor for ^{208}Pb plotted over a range of 0 to 0.5 fm^{-1}. As it can be seen from the figure, the form factors are not significantly different to 0.4fm^{-1}. They differ by 45.06% at the momentum transfer 0.5 fm^{-1}.

Most significantly, in Fig. (3.2), the first diffraction minimum in the FB form factor and the second minimum in the analytical form factor with

rectangular shape density distribution occur close to about 8fm^{-1} whereas the first minimum in the analytical form factor with rectangular shape density distribution occurs at smaller momentum transfer about 4fm^{-1}.

Table (3.2) The Rectangular and FB form factors for ^{208}Pb

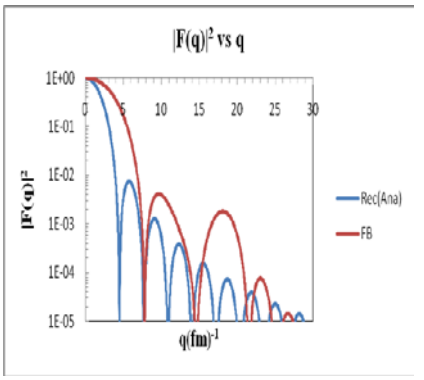

q	$\|F(q)\|^2$		
(fm^{-1})	Rectangular	FB	Percentage
5	3.26E-03	1.68E-01	98.06
10	5.54E-03	3.96E-03	86.01
15	1.15E-03	2.80E-05	97.57
20	7.39E-06	5.98E-04	98.76
25	2.29E-05	7.90E-07	96.55

Fig.(3.2)Rectangular and FB form factors for ^{208}Pb

Fig.(3.3) shows that at the low momentum transfers to 0.3fm^{-1} the rectangular(MoM) and Helm form factors for ^{208}Pb are nearly the same and then they begin to diverge from each other. Their form factor differences at the momentum transfers 0.1fm^{-1} and 0.5fm^{-1} are 0.33% and 57.02%, respectively.

Table (3.3) The Rectangular(MoM) and Helm form factors squared for ^{208}Pb

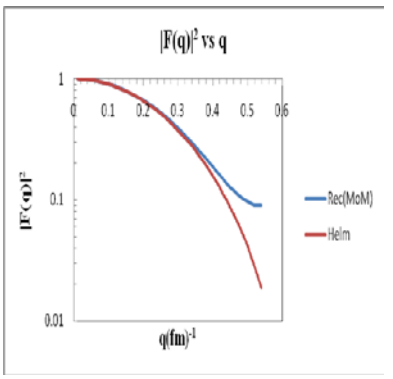

q	$\|F(q)\|^2$		
(fm^{-1})	Rectangular(MoM)	Helm	Percentage
0.1	0.9055	0.9025	0.33
0.2	0.6670	0.6582	1.32
0.3	0.3927	0.3770	4.00
0.4	0.1879	0.1587	15.54
0.5	0.0961	0.0413	57.02

Fig.(3.3) Rectangular(MoM) and Helm form factors for ^{208}Pb

In Fig. (3.4) Woods-Saxon (2pF) and MoM form factors for ^{208}Pb are not significantly different to 0.3fm^{-1}. Their form factor differences at the

momentum transfers $0.1fm^{-1}$ and $0.5fm^{-1}$ are 0.1% and 51.04%, respectively.

Table (3.4) The WS(2pF) and MoM form factor squared for ^{208}Pb

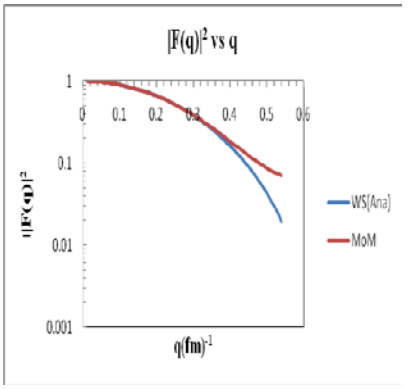

q	$\|F(q)\|^2$		
(fm^{-1})	WS(2pF)	MoM	Percentage
0.1	0.9044	0.9035	0.1
0.2	0.6628	0.6617	0.17
0.3	0.3825	0.3873	1.24
0.4	0.1623	0.1845	12.03
0.5	0.0423	0.0864	51.04

Fig.(3.4)WS(2pF) and MoM form factors for ^{208}Pb

Fig. (3.5) shows that Woods-Saxon (2pF) and SOG form factors for ^{208}Pb are nearly the same at smaller momentum transfer to $1fm^{-1}$ and then they begin to diverge from each other. The first minimum of Woods-Saxon (2pF) form factor for ^{208}Pb coincides with that of SOG form factors for ^{208}Pb. The second minimum of Woods-Saxon (2pF) form factor for ^{208}Pb is nearly the same with that of the SOG form factors for ^{208}Pb. Their form factor differences 0.84% and 19.88% are at the momentum transfers $0.1fm^{-1}$ and 0.5 fm^{-1}, respectively.

Table (3.5) The WS(2pF) and SOG form factors squared for ^{208}Pb

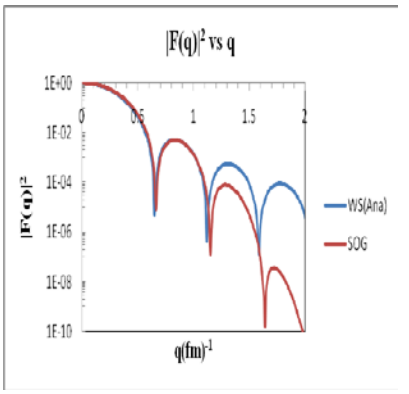

q	$\|F(q)\|^2$		
(fm^{-1})	WS(2pF)	SOG	Percentage
0.1	0.9044	0.9121	0.84
0.2	0.6628	0.6860	3.38
0.3	0.3825	0.4128	7.34
0.4	0.1623	0.1856	12.55
0.5	0.0423	0.0528	19.89

Fig.(3.5)WS(2pF) and SOG form factors for ^{208}Pb

Table (3.6) The WS(2pF) and Helm form factors squared for ^{208}Pb

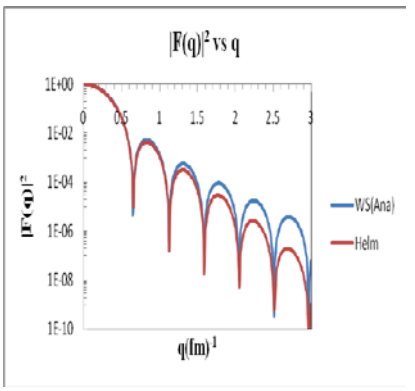

q	$\|F(q)\|^2$		
(fm^{-1})	WS(2pF)	Helm	Percentage
0.1	0.9044	0.9025	0.21
0.2	0.6628	0.6582	0.69
0.3	0.3825	0.3770	1.44
0.4	0.1623	0.1587	2.22
0.5	0.0423	0.0413	2.36

Fig.(3.6)WS(2pF) and Helm form form factors for ^{208}Pb

In Fig.(3.6), the maxima and minima of WS(2pF) form factors for ^{208}Pb are significantly same with those of Helm form factors for ^{208}Pb. Their form factor differences are fairly small.

Table (3.7) The Rectangular(MoM) and SOG form factors squared for ^{40}Ca

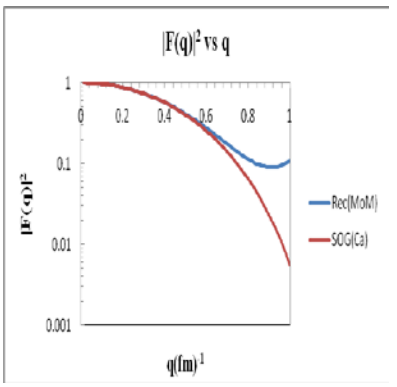

q	$\|F(q)\|^2$		
(fm^{-1})	Rectangular(MoM)	SOG	Percentage
0.1	0.9668	0.9671	0.03
0.2	0.8728	0.8735	0.08
0.3	0.7338	0.7335	0.04
0.4	0.5722	0.5684	0.66
0.5	0.4125	0.4015	2.67

Fig(3.7)Rectangular(MoM) and SOG form factors for ^{40}Ca

Fig. (3.7) shows the MoM form factor with rectangular shape density distribution and SOG form factor for ^{40}Ca plotted over a range of 0 to 1 fm^{-1}. It is shown that the form factors are not significantly different to 0.6 fm^{-1}. Afterward, they begin to diverge from each other at a momentum

transfer corresponding to 1fm^{-1}.Their form factors also differ by fairly small amount.

Table (3.8) The Rectangular and FB form factors squared for ^{40}Ca

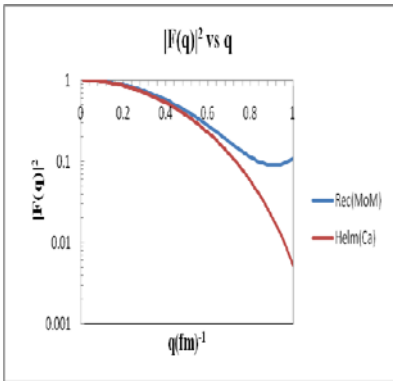

q	$\|F(q)\|^2$		
(fm^{-1})	Rectangular	FB	Percentage
5	3.26E-03	1.90E-01	98.28
10	5.54E-03	3.54E-04	93.61
15	1.15E-03	3.85E-05	96.65
20	7.39E-06	9.16E-06	19.32
25	2.29E-05	1.16E-08	99.95

Fig.(3.8)Rectangular and FB form factors for ^{40}Ca

In Fig. (3.8), the first diffraction minimum in the FB form factor for ^{40}Ca exists at the momentum transfer 10 fm^{-1} beyond the second minimum in the analytical form factor with rectangular shape density distribution.

Table (3.9)The Rectangular(MoM) and Helm form factors squared for ^{20}Ca

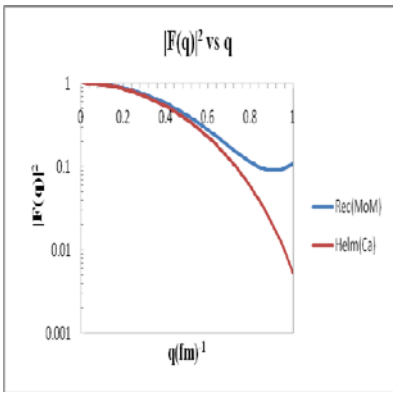

q	$\|F(q)\|^2$		
(fm^{-1})	Rectangular(MoM)	Helm	Percentage
0.1	0.9668	0.9622	0.48
0.2	0.8728	0.8565	1.87
0.3	0.7338	0.7034	4.14
0.4	0.5722	0.5306	7.27
0.5	0.4125	0.3649	11.54

Fig.(3.9)Rectangular(MoM) and Helm form factors for ^{40}Ca

Fig.(3.9) shows that at the low momentum transfers to 0.4 fm^{-1} the rectangular(MoM) and Helm form factors for ^{40}Ca are nearly the same and then they begin to diverge from each other. Their form factor differences 0.48% and 11.54% are at the momentum transfers 0.1fm^{-1} and 0.5fm^{-1}, respectively.

Table (3.10) The WS(2pF) and MoM form factors squared for ^{40}Ca

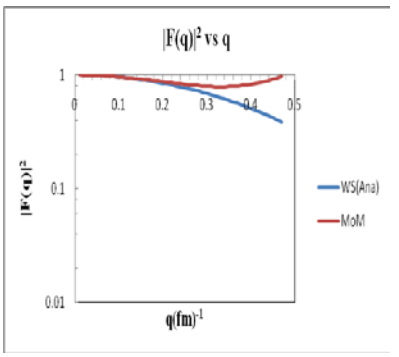

q	$\|F(q)\|^2$		
(fm^{-1})	WS(2pF)	MoM	Percentage
0.1	0.9604	0.9612	0.08
0.2	0.8480	0.8705	2.58
0.3	0.6865	0.7945	13.59
0.4	0.5064	0.8240	38.54
0.5	0.3367	1.0841	53.88

Fig.(3.10) WS(2pF) and MoM form factors for ^{40}Ca

In Fig. (3.10) Woods-Saxon (2pF) form factors for ^{40}Ca are significantly same with the MoM form factors for ^{40}Ca to the momentum transfer 0.2 fm^{-1}. They differ by 53.88% at the momentum transfer 0.5 fm^{-1}.

Table (3.11) The WS(MoM) and SOG form factors squared for ^{40}Ca

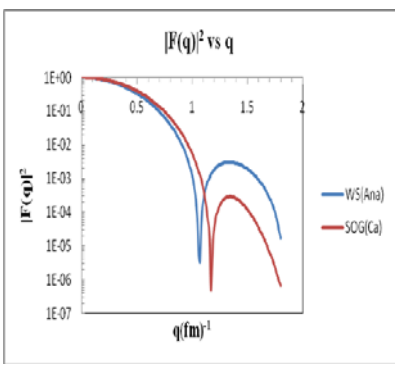

q	$\|F(q)\|^2$		
(fm^{-1})	WS(2pF)	SOG	Percentage
0.1	0.9604	0.9671	0.69
0.2	0.8480	0.8735	2.92
0.3	0.6865	0.7335	6.41
0.4	0.5064	0.5684	10.91
0.5	0.3367	0.4015	16.14

Fig.(3.11) WS(2pF) and SOG form factors for ^{40}Ca

Fig. (3.11) shows that Woods-Saxon (2pF) and SOG form factors for ^{40}Ca are nearly the same at smaller momentum transfer to 0.5 fm^{-1} and then they begin to diverge from each other. Their respective form factor differences at the momentum transfers 0.1fm^{-1} and 0.5 fm^{-1} are 0.69% and 16.14%.

Table (3.12) The WS(MoM) and Helm form factors squared for ^{40}Ca

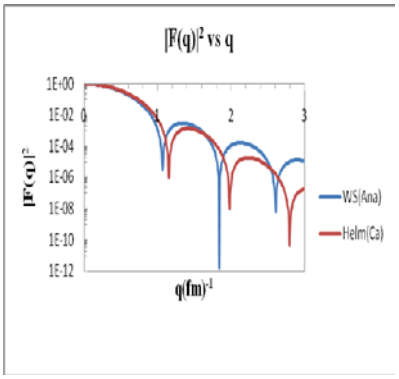

q (fm^{-1})	$\|F(q)\|^2$ WS(2pF)	Helm	Percentage
0.1	0.9604	0.9622	0.19
0.2	0.8480	0.8565	0.99
0.3	0.6865	0.7034	2.40
0.4	0.5064	0.5306	4.56
0.5	0.3367	0.3649	7.73

Fig.(3.12) WS(2pF) and Helm form factors for ^{40}Ca

The first minima of WS(2pF) and Helm form factors for ^{40}Ca shown in Fig.(3.12) nearly exist along the momentum transfer axis although the second minimum of WS(2pF) form factors for ^{40}Ca has a deep dip. Their form factor differences are fairly small.

Conclusion

The concept of nuclear form factor is now used widely in nuclear and particle physics to explore the effects of the spatial distribution of the interaction. In the lowest order Born approximation, the form factor is the Fourier transform of the nuclear mass distribution. The mass distribution of nuclei is not well known, and instead it is generally assumed that the nuclei's mass distribution is approximately the same as its charge distribution. In this work, the distributions considered are the rectangular-type distribution, Woods-Saxon (2pF) distribution and Helm distribution as model-dependent approaches and Fourier-Bessel (FB) and the Sum-of-Gaussian (SOG) fit as model-independent approaches.

The method of moment (MoM) for form factor depends on the influence of the higher nuclear moments, $\left\langle r^{2k} \right\rangle$ and is reliable for the smaller momentum transfers less than 1fm^{-1}. The rectangular type distribution of nuclear density is a non-physical model because of the abrupt cutoff mathematically imposed on it. In this work, the derivation of an analytic expression for the form factor of the two-parameter Fermi distribution is presented. The analytic expression consists of a simple term with elementary functions plus a rapidly convergent infinite series with terms of alternating sign. In the calculations in this work, the short expression, in which the summation terms are dropped out, is used with adequate accuracy. The Woods-Saxon or two parameter Fermi distribution is favored because it only has two parameters and they have been determined from nuclear scattering experiments. The analytic Helm form factor is obtained by convolving a constant, spherical charge distribution with a 'blurred' skin. In the Sum of Gaussians (SOG) expansion, the charge density of a nucleus is modeled as a series of Gaussians. It has a rapid fall-off of the Gaussian tail, and as long as a sufficient number of Gaussians are used it also ensures a good fit. The results of Fourier–Bessel (FB) expansion depend slightly on the value of the cut-off radius R. The Fourier–Bessel (FB) expansion and the Sum of Gaussians (SOG) expansion form factors have the advantage that they are model independent and analytics. Their use is simple and convenient.

All the form factor results show typical diffraction patterns, which reflect the internal structure of the nucleus. Although the form factor curves are similar in shape, they have different locations of maxima and minima along the momentum transfer ranges.

References

Blankenbecler, R. (1957) . Am. J. Phys. **25**, 279.

Dreher, et al. (1974). Nucl. Phys. **A 235** 219.

Duda, G. (2007) Nuclear Physics B (Proc. Suppl.) 173 68–71.

Fricke G. et al. (1995). Atomic Data and Nuclear Data Tables 60, 177-285.

Gustavsson, M. G. H. and Martensson-Pendrill A.-M. (1998). Advances in Quantum Chemistry **30**, 343-360.

Helm, R. (1956) Phys. Rev. 104 1466.

Lewin, J.D. and Smith, P.F. (1996) Astropart. 6 87.

Maximon L .C. and Schrack, R. A. (1966) JOURNAL OF RESEARCH of the National Bureau of Standards – B. Mathematics and Mathematical Physics Vol. 70B, No. 1, January – March.

Povh, B., Rith, K., Scholz, C., Zetsche, F. and Lavelle, M. (2008).Particles and Nuclei.

Sick, I. (1974). Nucl. Phys. **A 218** 509.